

DOI: 10.7511/jslx20171129003

# 金属结构航天器陨落过程三维瞬态 传热有限元算法研究

石卫波<sup>1</sup>, 孙海浩<sup>1</sup>, 唐小伟<sup>1</sup>, 马强<sup>3</sup>, 李志辉<sup>\*1,2</sup>

(1. 中国空气动力研究与发展中心, 绵阳 621000; 2. 国家计算流体力学实验室, 北京 100191;  
3. 四川大学 数学学院, 成都 610043)

**摘要:**构建金属桁架结构航天器陨落再入气动热环境有限元传热模型,是准确预测在轨服役期满大型航天器陨落再入解体过程温度分布的关键。本文采用四节点四面体单元对空间进行离散,依据泛函理论,将传热控制方程离散为代数方程组;利用有限单元法总体合成得到具有对称正定、高度稀疏和非0元素分布的规律性刚度矩阵,发展一维变带宽压缩存储技术,有效解决大型稀疏矩阵的数据存储问题;为有效抑制求解过程中出现的温度在时间和空间上的振荡问题,发展集中热容矩阵系数处理方法,将热容矩阵的同行或同列元素相加代替对角线元素,使非对角线元素化为0,构造求解三维瞬态温度场的两点向后差分格式、Crank-Nicolson格式和 Galerkin 格式。通过对正方体瞬态传热计算验证分析,在相同条件下,采用以上三种格式均可获得一致稳定的温度解,并得到与现有 ANSYS 有限元软件较为吻合的计算结果,验证了所建立三维瞬态传热有限元计算模型的准确可靠性。在此基础上,对铝合金低轨航天器薄壳结构进行了传热计算,给出了类天宫飞行器两舱体陨落飞行 107.5 km~90 km 不同高度的瞬态温度分布,为这类寿命末期航天器陨落再入解体预报提供理论支撑与可计算模型。

**关键词:**金属桁架结构航天器;陨落再入;三维瞬态传热;有限元计算模型

**中图分类号:** O343.6      **文献标志码:** A      **文章编号:** 1007-4708(2019)02-0219-07

## 1 引言

在轨运行的大型航天器任务完成后,将以高超声速陨落再入大气层,在与周围空气的压缩和剧烈摩擦中产生气动力/热冲击作用,航天器表面温度不断升高,将使金属材料变形软化/失效和复合材料热解/烧蚀以致解体<sup>[1-3]</sup>,对此陨落坠毁过程,准确预测大型金属桁架结构航天器表面温度分布是开展这类航天器寿命末期陨落再入过程分析及预报的关键<sup>[1,4,5]</sup>。

国外尤其是俄罗斯、美国和欧洲,有长期的航天飞行研究经历,在空间碎片再入解体预测方面积累了大量的经验,并形成了评估分析软件<sup>[2,6-9]</sup>。航天器结构热分析技术方面,大多数采用有限元方法<sup>[10-19]</sup>,也有采用有限体积法和边界元方法来求解。对于复杂结构构形,现已有复杂程度不一的模型来表征航天器的内部结构<sup>[13,20,21]</sup>。一般用三种

有限元模型,采用简单的一维有限元模型模拟结构厚度方向的传热<sup>[10,21-24]</sup>,在厚度方向上划分单元和节点,一维导热单元连接热防护板厚度方向上各节点。用各节点温度值的插值来近似模拟热防护板内的温度场分布。一维单元模型最大的缺点是忽略了与板平行的板缘和板间缝隙的热短路现象,于是提出了二维和三维有限元模型。目前,二维热模型不但对热防护结构沿厚度方向进行传热分析,而且对热防护结构剖面的其余方向也进行传热分析,同时还顾及边界条件的作用<sup>[13]</sup>。二维模型与一维模型相比虽复杂,但精确度较高。三维有限元模型可以模拟空间三个方向上的传热分析,但是也需要比简单模型更多的时间与计算量。三维模型可以模拟结构边缘和不连续热短路的影响<sup>[10]</sup>,如加强件以及通道和支撑框架,比简单模型更精确。

在轨服役期满航天器结构部件主要是桁架型金属或合金材料和一些嵌层使用的碳基复合材料,其热导率较高,三维传热效应明显。为了给出金属桁架结构航天器在强气动力/热致金属(合金)结构材料变形软化/失效、复合材料热解/烧蚀解体的理论预测<sup>[25-28]</sup>,需要开展三维传热模型研究<sup>[29-31]</sup>。非结构网格的三维有限元传热模型适用于尺寸大且外形复杂的铝合金薄壳两舱结构航天器的传热计

收稿日期:2017-11-29;修改稿收到日期:2018-02-05.

基金项目:国家重点基础研究发展计划(2014CB744100);国家自然科学基金(11325212;91530319)资助项目.

作者简介:石卫波(1972-),男,硕士,高级工程师;  
李志辉\*(1968-),男,博士,研究员  
(E-mail:zhli0097@x263.net).

算。为此,针对大型航天器陨落再入过程瞬态传热温度分布算法研究,本文在使用跨流域空气动力学模拟方法<sup>[33-35]</sup>计算航天器陨落再入过程气动热环境作为边界条件的基础上,开展铝合金结构热响应有限元建模与求解,并考虑金属材料表面熔融对传热的影响,建立适于金属桁架结构航天器再入瞬态传热有限元算法,实施航天器沿小再入角弹道飞行不同高度气动热环境致材料结构瞬态传热温度场的高精度数值计算,为金属桁架结构变形软化熔融和复合材料热解烧蚀模拟提供所需的温度条件与可计算模型。

## 2 有限元传热模型

### 2.1 三维有限元传热模型

在使用跨流域空气动力学模拟方法<sup>[5,33-35]</sup>计算航天器表面热流源项作为边界条件的情况下,三维瞬态热传导控制方程<sup>[11,27,28,35]</sup>为

$$\rho C_p \frac{\partial T}{\partial t} = \frac{\partial}{\partial x} \left[ k \frac{\partial T}{\partial x} \right] + \frac{\partial}{\partial y} \left[ k \frac{\partial T}{\partial y} \right] + \frac{\partial}{\partial z} \left[ k \frac{\partial T}{\partial z} \right] - \rho C_p \mathbf{V} \cdot \text{grad} T + Q \quad (1)$$

采用四面体四节点单元进行空间离散,求解三维温度场问题。四面体单元中任意一点的温度  $T$  可由  $i, j, m$  和  $l$  四个节点的温度  $T_i, T_j, T_m$  和  $T_l$  线性表示为

$$T(x, y, z, t) = N_i T_i + N_j T_j + N_m T_m + N_l T_l \quad (2)$$

式中  $N_i, N_j, N_m$  和  $N_l$  为形函数,其表达式为

$$N_g = \frac{1}{6V} (a_g + b_g x + c_g y + d_g z) \quad (g = i, j, m, l) \quad (3)$$

式中  $V$  为四面体单元的体积,  $a_g, b_g, c_g$  和  $d_g$  ( $g = i, j, m, l$ ) 是单元四个节点坐标的函数,其计算式分别表示为

$$V = \frac{1}{6} \begin{vmatrix} 1 & x_i & y_i & z_i \\ 1 & x_j & y_j & z_j \\ 1 & x_m & y_m & z_m \\ 1 & x_l & y_l & z_l \end{vmatrix} = \frac{1}{6} (a_i + a_j + a_m + a_l)$$

$$a_i = (-1)^{i+1} \begin{vmatrix} x_j & y_j & z_j \\ x_m & y_m & z_m \\ x_l & y_l & z_l \end{vmatrix}, \quad b_i = (-1)^i \begin{vmatrix} 1 & y_j & z_j \\ 1 & y_m & z_m \\ 1 & y_l & z_l \end{vmatrix}$$

$$c_i = (-1)^{i+1} \begin{vmatrix} 1 & x_j & z_j \\ 1 & x_m & z_m \\ 1 & x_l & z_l \end{vmatrix}, \quad d_i = (-1)^i \begin{vmatrix} 1 & x_j & y_j \\ 1 & x_m & y_m \\ 1 & x_l & y_l \end{vmatrix}$$

( $i, j, m, l = \overrightarrow{1, 2, 3, 4}$ )

温度场有限元法的平衡方程可从泛函变分求得。根据加权余量法,导出单元的平衡方程,对

第三类边界条件,适于三维空间温度场四面体有限单元法计算的基本方程为

$$\frac{\partial J^e}{\partial T_g} = \iiint_e \left\{ k \left[ \frac{\partial T}{\partial x} \frac{\partial}{\partial T_g} \left( \frac{\partial T}{\partial x} \right) + \frac{\partial T}{\partial y} \frac{\partial}{\partial T_g} \left( \frac{\partial T}{\partial y} \right) + \frac{\partial T}{\partial z} \frac{\partial}{\partial T_g} \left( \frac{\partial T}{\partial z} \right) \right] - Q \frac{\partial T}{\partial T_g} + \rho C_p \frac{\partial T}{\partial t} \frac{\partial T}{\partial T_g} + (\rho C_p \mathbf{V} \cdot \text{grad} T) \frac{\partial T}{\partial T_g} \right\} dx dy dz + \iint_{S_g} \alpha (T - T_f) \frac{\partial T}{\partial T_g} dS = 0 \quad (g = i, j, m, l) \quad (4)$$

对第二类边界条件,三维空间温度场四面体有限单元法计算的基本方程为

$$\frac{\partial J^e}{\partial T_g} = \iiint_e \left\{ k \left[ \frac{\partial T}{\partial x} \frac{\partial}{\partial T_g} \left( \frac{\partial T}{\partial x} \right) + \frac{\partial T}{\partial y} \frac{\partial}{\partial T_g} \left( \frac{\partial T}{\partial y} \right) + \frac{\partial T}{\partial z} \frac{\partial}{\partial T_g} \left( \frac{\partial T}{\partial z} \right) \right] - Q \frac{\partial T}{\partial T_g} + \rho C_p \frac{\partial T}{\partial t} \frac{\partial T}{\partial T_g} + (\rho C_p \mathbf{V} \cdot \text{grad} T) \frac{\partial T}{\partial T_g} \right\} dx dy dz + \iint_{S_g} q_n \frac{\partial T}{\partial T_g} dS = 0 \quad (g = i, j, m, l) \quad (5)$$

将式(2,3)分别代入式(4,5),即可求得四面体单元的有限元平衡方程为

$$[K]^e \{T\}^e + [N]^e \left\{ \frac{\partial T}{\partial t} \right\}^e + [v]^e \{T\}^e = \{P\}^e \quad (6)$$

式中 单元刚度矩阵中的各项系数为

$$k_{ii} = \frac{k}{36V} (b_i^2 + c_i^2 + d_i^2) + \frac{\Delta_{ijm}}{6} \alpha$$

$$k_{jj} = \frac{k}{36V} (b_j^2 + c_j^2 + d_j^2) + \frac{\Delta_{ijm}}{6} \alpha$$

$$k_{mm} = \frac{k}{36V} (b_m^2 + c_m^2 + d_m^2) + \frac{\Delta_{ijm}}{6} \alpha$$

$$k_{ll} = \frac{k}{36V} (b_l^2 + c_l^2 + d_l^2)$$

$$k_{ij} = k_{ji} = \frac{k}{36V} (b_i b_j + c_i c_j + d_i d_j) + \frac{\Delta_{ijm}}{12} \alpha$$

$$k_{im} = k_{mi} = \frac{k}{36V} (b_i b_m + c_i c_m + d_i d_m) + \frac{\Delta_{ijm}}{12} \alpha$$

$$k_{il} = k_{li} = \frac{k}{36V} (b_i b_l + c_i c_l + d_i d_l)$$

$$k_{jm} = k_{mj} = \frac{k}{36V} (b_j b_m + c_j c_m + d_j d_m) + \frac{\Delta_{ijm}}{12} \alpha$$

$$k_{jl} = k_{lj} = \frac{k}{36V} (b_j b_l + c_j c_l + d_j d_l)$$

$$k_{ml} = k_{lm} = \frac{k}{36V} (b_m b_l + c_m c_l + d_m d_l)$$

式中  $\Delta_{ijm}$  为三角形  $ijm$  的面积,  $k$  为材料的导热系数,  $V$  为单元体积,  $\alpha$  为对流传热系数。令  $\alpha = 0$ , 即可由上述各式得到第二类边界条件的单元刚度矩阵系数。

变温矩阵中的各项系数为

$$\begin{aligned} n_{ii} &= n_{jj} = n_{mm} = n_{ll} = \rho C_p V / 10 \\ n_{ij} &= n_{ji} = n_{im} = n_{mi} = n_{il} = n_{li} = n_{jm} = n_{mj} = \\ & n_{jl} = n_{lj} = n_{ml} = n_{lm} = \rho C_p V / 20 \end{aligned} \quad (7)$$

针对第三类边界条件,单元平衡方程(6)右端等效载荷系数为

$$p_i = p_j = p_m = \frac{V}{4} Q + \frac{\Delta_{ijm}}{3} \alpha T_f, \quad p_l = \frac{V}{4} Q \quad (8)$$

式中  $T_f$  为环境温度,  $Q$  为热源密度。

针对第二类边界条件,

$$p_i = p_j = p_m = \frac{V}{4} Q - \frac{\Delta_{ijm}}{3} q_n, \quad p_l = \frac{V}{4} Q \quad (9)$$

考虑物面热源边界影响,热容矩阵中的各项系数为

$$\begin{aligned} \begin{bmatrix} \nu_{ii} & \nu_{ij} & \nu_{im} & \nu_{il} \\ \nu_{ji} & \nu_{jj} & \nu_{jm} & \nu_{jl} \\ \nu_{mi} & \nu_{mj} & \nu_{mm} & \nu_{ml} \\ \nu_{li} & \nu_{lj} & \nu_{lm} & \nu_{ll} \end{bmatrix} &= \frac{\rho C_p}{120} \begin{bmatrix} 2 & 1 & 1 & 1 \\ 1 & 2 & 1 & 1 \\ 1 & 1 & 2 & 1 \\ 1 & 1 & 1 & 2 \end{bmatrix} \cdot \\ \begin{cases} \nu_{ix} \\ \nu_{jx} \\ \nu_{mx} \\ \nu_{lx} \end{cases} & \left[ \begin{matrix} b_i & b_j & b_m & b_l \end{matrix} \right] + \frac{\rho C_p}{120} \begin{bmatrix} 2 & 1 & 1 & 1 \\ 1 & 2 & 1 & 1 \\ 1 & 1 & 2 & 1 \\ 1 & 1 & 1 & 2 \end{bmatrix} \cdot \\ \begin{cases} \nu_{iy} \\ \nu_{jy} \\ \nu_{my} \\ \nu_{ly} \end{cases} & \left[ \begin{matrix} c_i & c_j & c_m & c_l \end{matrix} \right] + \frac{\rho C_p}{120} \begin{bmatrix} 2 & 1 & 1 & 1 \\ 1 & 2 & 1 & 1 \\ 1 & 1 & 2 & 1 \\ 1 & 1 & 1 & 2 \end{bmatrix} \cdot \\ \begin{cases} \nu_{iz} \\ \nu_{jz} \\ \nu_{mz} \\ \nu_{lz} \end{cases} & \left[ \begin{matrix} d_i & d_j & d_m & d_l \end{matrix} \right] \end{aligned}$$

所有四面体有限单元按式(6)进行总体合成(同一单元中的相邻节点在合成时会对该点方程的系数值有所贡献,而不在同一单元中的其余节点就不会贡献),并将物面边界热源项影响加入到温度刚度矩阵中,最后得到  $n$  个代数方程,把这个方程组写成矩阵形式:

$$\begin{bmatrix} k_{11} & k_{12} & \cdots & k_{1n} \\ k_{21} & k_{22} & \cdots & k_{2n} \\ \cdots & \cdots & \cdots & \cdots \\ k_{n1} & k_{n2} & \cdots & k_{nn} \end{bmatrix} \cdot \begin{bmatrix} T_1 \\ T_2 \\ \vdots \\ T_n \end{bmatrix}_t + \begin{bmatrix} n_{11} & n_{12} & \cdots & n_{1n} \\ n_{21} & n_{22} & \cdots & n_{2n} \\ \cdots & \cdots & \cdots & \cdots \\ n_{n1} & n_{n2} & \cdots & n_{nn} \end{bmatrix} \cdot \begin{bmatrix} p_1 \\ p_2 \\ \vdots \\ p_n \end{bmatrix}_t = \begin{bmatrix} \partial T_1 / \partial t \\ \partial T_2 / \partial t \\ \vdots \\ \partial T_n / \partial t \end{bmatrix}_t$$

或简写为

$$[K] \{T\}_t + [N] \left\{ \frac{\partial T}{\partial t} \right\}_t = \{P\}_t \quad (10)$$

## 2.2 三维瞬态温度场的有限单元方程数值求解格式

在求解三维瞬态温度场时,通常已知的是边界条件和初始条件,  $\{\partial T / \partial t\}_t$  未知,在利用式(10)求解  $\{T\}_t$  时,要用差分法把  $\{\partial T / \partial t\}_t$  展开。差分后的有限元法计算瞬态温度场的基本方程可分别使用如下三种方案<sup>[11]</sup>,

向后差分格式:

$$\left[ [K] + \frac{[N]}{\Delta t} \right] \{T\}_t = \{P\}_t + \frac{[N]}{\Delta t} \{T\}_{t-\Delta t} \quad (11)$$

Crank-Nicolson 格式:

$$\begin{aligned} \left[ [K] + \frac{2[N]}{\Delta t} \right] \{T\}_t &= (\{P\}_t + \{P\}_{t-\Delta t}) + \\ & \left[ \frac{2[N]}{\Delta t} - [K] \right] \{T\}_{t-\Delta t} \end{aligned} \quad (12)$$

Galerkin 格式:

$$\begin{aligned} \left[ 2[K] + \frac{3[N]}{\Delta t} \right] \{T\}_t &= (2\{P\}_t + \{P\}_{t-\Delta t}) + \\ & \left[ \frac{3[N]}{\Delta t} - [K] \right] \{T\}_{t-\Delta t} \end{aligned} \quad (13)$$

在数值求解过程中,为有效克服方程离散求解出现在时间和空间上的振荡现象,采取将热容矩阵系数集中的办法<sup>[17]</sup>,将热容矩阵的同行或同列元素相加代替对角线元素,使其非对角线元素化为0。于是,新的热容矩阵只有对角线的元素,其余元素均为0。由于有限单元法总体合成得到的刚度矩阵具有对称正定、高度稀疏和非0元素分布的规则性,采用一维变带宽技术压缩存储三角阵中的非0元素。应用共轭梯度法<sup>[36]</sup>求解该大型稀疏对称正定方程组,得到所求温度场,由此建立求解金属桁架结构航天器陨落再入过程结构热响应瞬态温度场分布的数值计算方法。

## 3 方法验证与计算分析

### 3.1 三维有限元传热温度场计算模型验证

为考核三维有限元传热温度场分布计算模型的可靠性,以边长 10 mm 正方体作为研究对象,正方体材料物性参数为,密度 7850 kg/m<sup>3</sup>,比热 460 J/(kg·K),导热系数 59 W/(m·K),发射率 0.3;初始温度为 275 K,正方体一面施加恒定热流 1.5×10<sup>6</sup> W/m<sup>2</sup>,加热时间 200 s,另外 5 个面绝热。图 1 为分别使用式(11~13)计算得到的正方

体加热表面中心点处的热响应瞬态温度分布。计算结果表明,在相同计算条件下,采取将热容矩阵系数集中,分别使用两点向后差分格式、Crank-Nicolson 格式和 Galerkin 格式均可获得稳定的热响应温度解,其结果与 ANSYS 软件有限元热分析(采用 surf152, solid70 单元)计算结果吻合较好,而且本文三种格式计算结果几乎完全重合,说明本文算法模型的实现正确合理,证实由此形成的热响应温度场预测方法可靠。

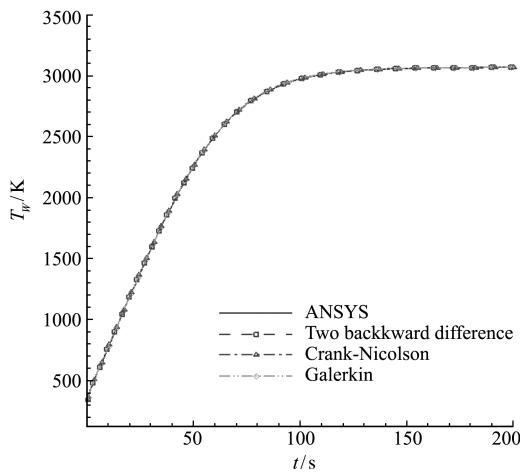
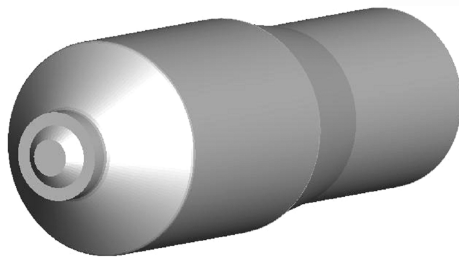
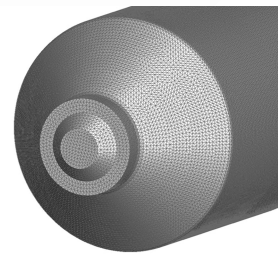


图 1 正方体加热表面中心点瞬态温度随时间变化  
Fig. 1 Transient temperature varies with the time at heating face center point of cube



(a) 复杂外形航天器几何构型  
(a) Complex spacecraft geometry configuration



(b) 传热计算网格(局部放大图)  
(b) Heat transfer calculation grid (local enlarged drawing)

图 2 两舱结构体航天器几何外形及传热计算网格  
Fig. 2 Two-capsule structure spacecraft geometry shape and heat transfer calculation grid

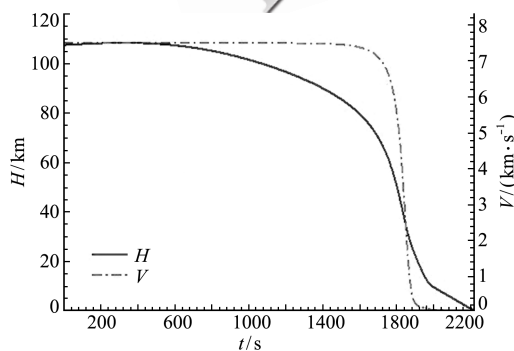


图 3 两舱结构体航天器再入弹道  
Fig. 3 Reentry trajectory of spacecraft with two-capsule structure

### 3.2 金属桁架结构航天器三维瞬态传热计算分析

拟定图 2(a)所示寿命末期低轨航天器陨落再入首次解体形成两舱结构体,该航天器外壳材料为铝合金,实验舱体厚度为 3.5 mm,资源舱体厚度为 1 mm;材料物性参数如下,密度为 2800 kg/m<sup>3</sup>,比热为 921 J/(kg·K),导热系数为 121 W/(m·K),熔化温度为 873 K<sup>[32]</sup>。根据跨流域空气动力学模拟方法<sup>[33-35]</sup>提供陨落飞行某高度飞行器表面热流数据,采用本文建立的三维有限元传热模型,对该铝合金薄壳结构航天器从 107.5 km~90 km 沿小再入角弹道(如图 3 所示,初始再入速度为 7.5 km/s)进行了气动热环境下的传热计算。计算过程中,金属材料采用熔点控制模型,即达到熔点 873 K 后金属将发生熔解吸热,表面温度保持在熔点。本文暂未考虑金属熔融导致的外形变化。图 4 为航天器以 0° 攻角陨落飞行到第 459 s 时的表面温度分布云图,可以看出,该航天器驻点局部区域表面温度已达到铝合金熔点。图 5 和图 6 分别为该航天器陨落飞行到第 801 s 和 1401 s 时的表面温度分布云图。计算结果表明,该两舱结构体低轨航天器以 0° 攻角高超声速陨落再入,将在 90 km 高度以上发生熔融解体,解体最先发生在迎风端面驻点区。

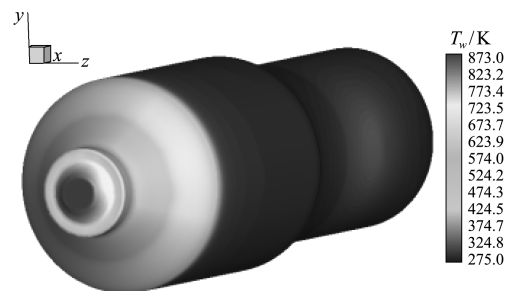


图 4 两舱结构体航天器在第 459 s 时表面温度分布云图  
Fig. 4 Surface temperature distribution of two-capsule structure spacecraft at 459 s



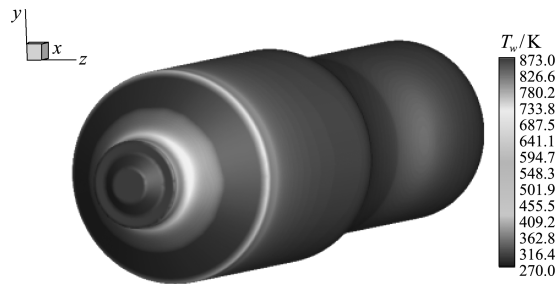


图5 两舱结构体航天器在第801 s时表面温度分布云图  
Fig. 5 Surface temperature distribution of two-capsule structure spacecraft at 801 s

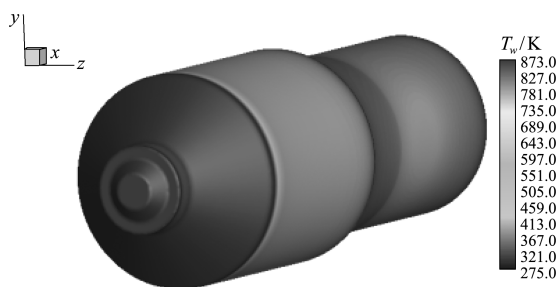


图6 两舱结构体航天器在第1401 s时表面温度分布云图  
Fig. 6 Surface temperature distribution of two-capsule structure spacecraft at 1401 s

#### 4 结 论

为了发展适于金属桁架结构大型航天器陨落再入过程的气动热环境结构响应瞬态温度场有限元算法应用研究平台,作为初步研究,本文以类天宫飞行器寿命末期限落再入首次解体形成的两舱结构体为研究对象,从三维瞬态热传导方程出发,提出四面体四节点有限单元法求解航天器表面结构温度场,使用泛函变分导出有限单元法结构热响应平衡方程。基于有限单元法总体合成使刚度矩阵具有对称正定、高度稀疏和非0元素分布的规则性,发展一维变带宽存储技术,解决大型稀疏矩阵的数据存储问题;应用集中变温矩阵系数的方法,有效抑制求解过程中的温度振荡现象,由此建立了一套适于金属桁架结构航天器陨落再入热响应温度场有限元计算模型。

研究表明,本文建立的金属桁架结构航天器再入三维瞬态传热有限元模拟方法及结果合理可行,已初步具备将跨流域空气动力学模拟方法<sup>[33-35]</sup>计算得到的气动热环境作为输入条件,进行金属桁架结构热响应瞬态传热计算的能力。下一步将围绕提高算法鲁棒性和大尺度复杂结构航天器的有攻角飞行绕流适应性模拟研究,建立强气动力热环境致金属桁架结构动态热力响应变形失效破坏一体化计算平台<sup>[27,28,36,38]</sup>,并根据结构温度分布,利用熔点控制模型对金属桁架结构航天器变形软化熔融解体过程进行计算分析预报。

#### 参考文献(References):

- [1] Hoyt R P, Forward R L. Performance of the Terminator Tether for autonomous deorbit of LEO spacecraft [A]. 35<sup>th</sup> AIAA/ASME/SAE/ASEE Joint Propulsion Conference & Exhibit[C]. 1999.
- [2] 丹 枫. 和平号的成功坠毁及其影响[J]. 国际太空, 2001(5): 6-8. (DAN Feng. The successful crash of Mir and its impact[J]. *International Space*, 2001(5): 6-8. (in Chinese))
- [3] Reyhanoglu M, Alvarado J. Estimation of debris dispersion due to a space vehicle breakup during reentry [J]. *Acta Astronautica*, 2013, **86**: 211-218.
- [4] Balakrishnan D, Kurian J. Material thermal degradation under reentry aerodynamic heating [J]. *Journal of Spacecraft and Rockets*, 2014, **51**(4): 1319-1328.
- [5] 李志辉, 梁 杰, 唐志共, 等. “航天飞行器跨流域空气动力学与飞行控制关键基础问题研究”项目 2014 年度进展报告[R]. 国家科技报告, 2014. (LI Zhi-hui, LIANG Jie, TANG Zhi-gong, et al. Progress in 2014 for “Study on Key Basic Problems of Aerodynamics and Flight Control Covering Flow Regimes for Aerospace Craft” [R]. National Science and Technology Report, 2014. (in Chinese))
- [6] Anonymous. DAS user's guide, version 2. 0 [R]. NASA, JSC-64047, 2007.
- [7] Bouslog S A, Ross B P, Madden C B. Space debris reentry risk analysis [A]. 32<sup>nd</sup> Aerospace Sciences Meeting & Exhibit[C]. 1994.
- [8] Fritsche B, Klinkrad H, Kashkovsky A, et al. Spacecraft disintegration during uncontrolled atmospheric re-entry [J]. *Acta Astronautica*, 2000, **47**(2-9): 513-522.
- [9] Lips T, Fritsche B. A comparison of commonly used re-entry analysis tools [J]. *Acta Astronautica*, 2005, **57**(2-8): 312-323.
- [10] Tamma K K, Thornton E A. Re-entry thermal/structural finite-element modeling/analysis of shuttle wing configurations [J]. *Journal of Spacecraft and Rockets*, 1987, **24**(2): 101-108.
- [11] 孔祥谦. 有限单元法在传热学中的应用(第三版) [M]. 北京: 科学出版社, 1998. (KONG Xiang-qian. *Application of Finite Element Method in Heat Transfer* (Third Edition) [M]. Beijing: Science Press, 1998. (in Chinese))
- [12] Gould D C. Thermal analysis of a high-speed aircraft wing using p-version finite elements [A]. 39<sup>th</sup> AIAA Aerospace Sciences Meeting & Exhibit[C]. 2001.
- [13] Blosser M. L. Investigation of fundamental modeling and thermal performance issues for a metallic thermal protection system design [A]. 40<sup>th</sup> AIAA Aerospace Sciences Meeting & Exhibit[C]. 2002.
- [14] 姜贵庆. 非烧蚀热防护与非烧蚀机理 [A]. 中国空气动力学学会近代空气动力学研讨会 [C]. 2005. (JIANG Gui-qing. Non-ablative thermal protection and non-

- ablative mechanism [A]. Symposium on Modern Aerodynamics of China Aerodynamics Society [C]. 2005. (in Chinese))
- [15] 马玉娥. 可重复使用运载器热防护系统热/力耦合数值计算研究[D]. 西北工业大学, 2005. (MA Yu-e. Study of Thermo-Mechanical Coupled Computation for Thermal Protection System of Reusable Launch Vehicle[D]. Northwestern Polytechnical University, 2005. (in Chinese))
- [16] 耿湘人, 桂业伟, 贺立新, 等. 红外窗口不同冷却方式下的结构传热和热应力特性计算研究[J]. 空气动力学学报, 2008, **26**(3): 329-333. (GENG Xiang-ren, GUI Ye-wei, HE Li-xin, et al. Numerical study on heat transfer and thermal stress for infra-window with externally cooled and internally cooled techniques [J]. *Acta Aerodynamica Sinica*, 2008, **26**(3): 329-333. (in Chinese))
- [17] 刘 刚, 李长生, 刘相华. 有限元法求解瞬态温度场时的振荡问题[J]. 钢铁研究学报, 2008, **20**(7): 19-22. (LIU Gang, LI Chang-sheng, LIU Xiang-hua. Oscillation problem during solving for transient temperature field using FEM [J]. *Journal of Iron and Steel Research*, 2008, **20**(7): 19-22. (in Chinese))
- [18] Ng W H, Friedmann P P, Waas A M. Thermomechanical behavior of a damaged thermal protection system: Finite-element simulations [J]. *Journal of Aerospace Engineering*, 2012, **25**(1): 90-102.
- [19] 张 涛, 孙 冰. 航天器再入全过程轴对称烧蚀热防护数值仿真研究[J]. 宇航学报, 2011, **32**(5): 1195-1204. (ZHANG Tao, SUN Bing. Numerical simulation research on axis-symmetrical ablative thermal protection for spacecraft in whole reentry[J]. *Journal of Astronautics*, 2011, **32**(5): 1195-1204. (in Chinese))
- [20] Blosser M L, Poteet C C, Chen R R, et al. Development of advanced metallic thermal protection system prototype hardware[J]. *Journal of Spacecraft and Rockets*, 2004, **41**(2): 183-194.
- [21] 闫长海, 孟松鹤, 陈贵清, 等. 金属热防护系统隔热材料的发展与现状[J]. 导弹与航天运载技术, 2006(4): 48-52. (YAN Chang-hai, MENG Song-he, CHEN Gui-qing, et al. Development of insulations for metallic thermal protection system and its current status [J]. *Missile and Space Vehicle*, 2006(4): 48-52. (in Chinese))
- [22] Darjabeigi K. Design of High Temperature Multi-layer Insulation for Reusable Launch Vehicles[D]. University of Virginia, 2000.
- [23] 张洪武, 付振东. 考虑辐射效应的多孔材料传热有限元算法[J]. 航空动力学报, 2005, **20**(1): 98-103. (ZHANG Hong-wu, FU Zhen-dong. Finite element method for heat conduction analysis in porous media with consideration of radiative effects[J]. *Journal of Aerospace Power*, 2005, **20**(1): 98-103. (in Chinese))
- [24] 熊启林, 田晓耕, 沈亚鹏, 等. 瞬态热冲击下层合材料板界面的热弹性行为[J]. 力学学报, 2011, **43**(3): 630-634. (XIONG Qi-lin, TIAN Xiao-geng, SHEN Ya-peng, et al. Thermoelastic behavior of interface of composite plate under thermal shock [J]. *Chinese Journal of Theoretical and Applied Mechanics*, 2011, **43**(3): 630-634. (in Chinese))
- [25] 国义军. 炭化材料烧蚀防热的理论分析与工程应用[J]. 空气动力学学报, 1994, **12**(1): 94-100. (GUO Yi-jun. An analysis of a charring ablative thermal protection system with its engineering application[J]. *Acta Aerodynamica Sinica*, 1994, **12**(1): 94-100. (in Chinese))
- [26] 唐小伟, 张顺玉, 党雷宁, 等. 非常规再入/进入问题探讨[J]. 航天返回与遥感, 2015, **36**(6): 11-21. (TANG Xiao-wei, ZHANG Shun-yu, DANG Lei-ning, et al. Discussion on unconventional reentry/entry [J]. *Spacecraft Recovery & Remotesensing*, 2015, **36**(6): 11-21. (in Chinese))
- [27] Li Z H, Ma Q, Cui J Z. Finite element algorithm for dynamic thermoelasticity coupling problems and application to transient response of structure with strong aerothermodynamic environment[J]. *Communications in Computational Physics*, 2016, **20**(3): 773-810.
- [28] Ma Q, Cui J Z, Li Z H, et al. Second-order asymptotic algorithm for heat conduction problems of periodic composite materials in curvilinear coordinates [J]. *Journal of Computational & Applied Mathematics*, 2016, **306**: 87-115.
- [29] 申跃奎, 赵德顺, 王 泰. 考虑流固耦合作用的充气膜结构风压分布研究[J]. 计算力学学报, 2017, **34**(5): 665-671. (SHEN Yue-kui, ZHAO De-shun, WANG Qin. On wind pressure coefficient distribution of air-supported structures considering fluid-structure coupling[J]. *Chinese Journal of Computational Mechanics*, 2017, **34**(5): 665-671. (in Chinese))
- [30] Collier CS. Thermoelastic formulation of stiffened, unsymmetric composite panels for finite element analysis of high speed aircraft [A]. AIAA/ASME/ASCE/AHS/ACS 35<sup>th</sup> Structures, Dynamics & Materials Conference [C]. 1994.
- [31] Thornton E A, Dechaumphai P, Wieting A R, et al. Integrated transient thermal-structural finite element analysis [A]. Proceedings of the AIAA/ASME/ASCE/AHS 22<sup>nd</sup> Structures, Structural Dynamics and Material Conference [C]. 1981.
- [32] 张顺玉, 唐小伟. 某大型航天器陨落过程初步研究 [A]. 第三届进入、减速、着陆(EDL)技术全国学术会议 [C]. 长沙, 2015. (ZHANG Shun-yu, TANG Xiao-wei. Preliminary study on the falling process of a large spacecraft [A]. 3<sup>rd</sup> National Academic Conference on Entry, Deceleration and Landing (EDL) Technology [C]. Changsha, 2015. (in Chinese))
- [33] 梁 杰, 李志辉, 杜波强, 等. 大型航天器再入陨落时

- 太阳翼气动力/热模拟分析[J]. 宇航学报, 2015, **36**(12): 1348-1355. (LIANG Jie, LI Zhi-hui, DU Bo-qiang, et al. Modeling and analysis of solar array aerothermodynamics during large-scale spacecraft reentry [J]. *Journal of Astronautics*, 2015, **36**(12): 1348-1355. (in Chinese))
- [34] 李中华,李志辉,李海燕,等. 过渡流区 N-S/DSMC 耦合计算研究[J]. 空气动力学学报, 2013, **31**(3): 282-287. (LI Zhong-hua, LI Zhi-hui, LI Hai-yan, et al. Research on CFD/DSMC hybrid numerical method in rarefied flows [J]. *Acta Aerodynamica Sinica*, 2013, **31**(3): 282-287. (in Chinese))
- [35] 李志辉,蒋新宇,吴俊林,等. 转动非平衡玻尔兹曼模型方程统一算法与全流域绕流计算应用[J]. 力学学报, 2014, **46**(3): 336-351. (LI Zhi-hui, JIANG Xin-yu, WU Jun-lin, et al. Gas-kinetic unified algorithm for Boltzmann model equation in rotational nonequilibrium and its application to the whole range flow regimes [J]. *Chinese Journal of Theoretical and Applied Mechanics*, 2014, **46**(3): 336-351. (in Chinese))
- [36] Li Z H, Ma Q, Cui J Z. Second-order two-scale finite element algorithm for dynamic thermo-mechanical coupling problem in symmetric structure [J]. *Journal of Computational Physics*, 2016, **314**: 712-748.
- [37] 丁丽娟,程杞元. 数值计算方法(第二版)[M]. 北京: 北京理工大学出版社, 2005. (DING Li-juan, CHENG Qi-yuan. *Numerical Methods* (2<sup>nd</sup> Edition) [M]. Beijing: Beijing University of Technology Press, 2005. (in Chinese))
- [38] Ma Q, Cui J Z, Li Z H. Second-order two-scale asymptotic analysis for axisymmetric and spherical symmetric structure with periodic configurations [J]. *International Journal of Solid and Structures*, 2016, **78-79**: 77-100.

## Study on finite element algorithm for three dimensional transient heat transfer during falling reentry of spacecraft with metal truss structure

SHI Wei-bo<sup>1</sup>, SUN Hai-hao<sup>1</sup>, TANG Xiao-wei<sup>1</sup>, MA Qiang<sup>3</sup>, LI Zhi-hui<sup>\*1,2</sup>

(1. China Aerodynamics Research and Development Center, Mianyang 621000, China;

2. National Laboratory for Computational Fluid Dynamics, Beijing 100191, China;

3. College of Mathematics, Sichuan University, Chengdu 610043, China)

**Abstract:** To construct the finite element model for the heat transfer of large-scale complex spacecraft with a metal truss structure during in reentry in aerothermodynamic environment, is the key to accurately predict the temperature distribution of the end-of-life spacecraft during the process of falling reentry and disintegration. In this paper, the four-node tetrahedron element is used to discretize the space, and the heat transfer equation is discretized into a set of algebraic equations. The symmetric positive-definite stiffness matrix with a highly sparse and non-zero element distribution is obtained by the overall synthesis of the finite element method. The one-dimensional variable bandwidth storage technique is developed to effectively resolve the data storage of large sparse matrix. To effectively depress the temperature oscillations appearing in time and space in the solving process, the centralized heat capacity matrix coefficient method is developed. The elements on the same row or column elements of the heat capacity matrix are summed to replace the diagonal elements, so that only the diagonal elements of the new heat capacity matrix are non-zero, and the remaining elements are zero. The two-point backward difference scheme, Crank-Nicolson scheme and Galerkin scheme are constructed to solve the three-dimensional transient temperature field. By computational analysis of transient heat transfer of a rectangular cylinder body, the converged temperature solutions of the above-said three schemes are found to be in good agreement, and the results are consistent with those of the existing finite-element software ANSYS, which confirms the precision and reliability of the present 3D finite-element model for transient heat transfer. The heat transfer computation is carried on the shell structure of a low-orbit spacecraft made of aluminium alloy, and the transient temperature distribution of the Tiangong's two-capsule structure is simulated and analyzed from the flight altitude of 107.5 km~90 km, which provides the theoretical support and computable model for the forecast of disintegration of the end-of-life spacecraft during falling reentry.

**Key words:** spacecraft with metal truss structure; falling reentry from the outer space; 3-dimensional transient heat transfer; finite-element computational model

引用本文/Cite this paper:

石卫波,孙海浩,唐小伟,等. 金属结构航天器陨落过程三维瞬态传热有限元算法研究[J]. 计算力学学报, 2019, **36**(2): 219-225.

SHI Wei-bo, SUN Hai-hao, TANG Xiao-wei, et al. Study on finite element algorithm for three dimensional transient heat transfer during falling reentry of spacecraft with metal truss structure [J]. *Chinese Journal of Computational Mechanics*, 2019, **36**(2): 219-225.